*Molecular Physics*, Vol. 103, Nos. 21–23, 10 November–10 December 2005, 3141–3151



# Phase transitions in equilibrium systems: microscopic models and mesoscopic free energies†

E. A. CARLEN‡, M. C. CARVALHO*§, R. ESPOSITO¶, J. L. LEBOWITZ†† and R. MARRA‡‡

‡School of Mathematics, Georgia Institute of Technology, Atlanta, GA 30332–0160, USA
§Department of Mathematics and GFM, University of Lisbon, 1649-003 Lisbon Portugal
¶Dip. di Matematica pura ed applicata, Università di L'Aquila, Coppito, 67100 AQ, Italy
††Departments of Mathematics and Physics, Rutgers University, New Brunswick, NJ 08903, USA
‡‡Dipartimento di Fisica and INFN, Università di Roma, Tor Vergata, 00133 Roma, Italy

(*Received 6 May 2005; in final form 9 June 2005*)

We describe the derivation of mesoscopic free energy functionals for systems with long-range Kac potentials and analyse them in the presence of phase transitions. This yields information about the arrangement of phases in some binary mixtures as well as explicit criteria for the stability of liquid droplets in a one-component fluid described by a Cahn–Hilliard type of free energy functional.

## 1. Introduction

Statistical mechanics provides a complete microscopic theory of phase transitions in equilibrium systems. While this is well understood in principle, it is a formidable and largely incomplete task to derive mathematically precise quantitative information about the phase diagram or surface tension of a system from its microscopic Hamiltonian. Information available for realistic effective Hamiltonians is generally of two types: it is either derived rigorously but is only qualitative, or else it is quantitative but based on approximations whose validity is difficult to assess. Examples of the former are the existence of convex free energy densities for macroscopic systems (formally in the infinite volume thermodynamic limit) which are analytic (no phase transitions) in the density $\rho$ and temperature $\beta^{-1}$ when $\rho$ and $\beta$ are sufficiently small [1]. Examples of the second kind are mean-field equations of state and integral equations for the structure function of fluids. An intermediate approach is to consider idealized model systems. When used judiciously, these models can provide useful information about the behaviour of real systems.

Ben Widom has made seminal contributions to statistical mechanics and thermodynamics by developing and utilizing simple models for elucidating complex phenomena. He has also been a great contributor to and expositor of clear thinking and mathematical precision in dealing with the complex phenomena which occur when several phases coexist. We dedicate this paper to him in appreciation and friendship.

### 1.1. *Statistical mechanical origin of mesoscopic free energies*

Our starting point here is a class of microscopic models of systems of particles interacting with a pair potential consisting of two parts: a short-range potential $U(r_{ij})$ and an attractive long-range, Kac-type, pair potential $J_\gamma(r_{ij}) = \gamma^d J(\gamma r_{ij})$, where $r_{ij}$ is the distance between particles $i$ and $j$, $d$ is the space dimension and $\gamma^{-1}$ is a length scale which is large compared to the interparticle distances. Consider a system of $N$ particles of mass $m$ in a region $\Omega \in \mathbb{R}^d$, with volume $|\Omega|$, interacting through such a pair potential. At inverse temperature $\beta$, the canonical partition function for the system is given by

$$Z(\beta, N, \Omega) = \frac{(2\pi m/\beta h^2)^{d(N/2)}}{N!} \times \int \exp\Big\{-\beta \sum \big[U(r_{ij}) + J_\gamma(r_{ij})\big]\Big\} \mathrm{d}r_1 \cdots \mathrm{d}r_N, \tag{1}$$

where $h$ is Planck's constant.

In the thermodynamic limit, i.e. letting $N$ and $|\Omega|$ go to infinity while $N/|\Omega| \to n$, some fixed average particle

*Corresponding author. Email: mcarvalh@cii.fc.ul.pt
†Dedicated to Ben Widom.

*Molecular Physics*
ISSN 0026–8976 print/ISSN 1362–3028 online © 2005 Taylor & Francis
http://www.tandf.co.uk/journals
DOI: 10.1080/00268970500221990

density, we obtain the Helmholtz free energy density $f(n,\gamma)$ [1],

$$f(n,\gamma) = -\lim_{|\Omega|\to\infty}\left[\frac{\beta^{-1}\log Z(N,\Omega)}{|\Omega|}\right], \tag{2}$$

with $f(n,\gamma)$ a convex function of $n$ whose dependence on $\beta$ is not indicated explicitly. The conditions on $U$ and $J$ necessary for the validity of this are very mild [1, 2].

Taking now the van der Waals limit $\gamma \to 0$, we obtain a formula for the Helmholtz free energy density in which the separate contributions of $U$ and $J$ are clearly displayed and the Gibbs double-tangent construction naturally enters [2]:

$$f(n) = \lim_{\gamma\to 0} f(n,\gamma) = CE\left[f_s(n) + \frac{1}{2}\alpha n^2\right]. \tag{3}$$

In (3), $f_s(n)$ is the free energy density of a system interacting only via the short range interactions $U(r)$, i.e. with $J_\gamma(r) = 0$,

$$\alpha = \int_{\mathbb{R}^d} J(r)\,\mathrm{d}r, \tag{4}$$

and $CE$ denotes the convex envelope (Gibbs double-tangent construction) applied to the mean field free energy $f_s(n) + \frac{1}{2}\alpha n^2$.

This will yield a first-order phase transition (vapour–liquid) when $\alpha$ is sufficiently negative, i.e. when

$$\alpha \le -\frac{\mathrm{d}^2}{\mathrm{d}n^2} f_s(n)$$

for some range of $n$. For details see [2, 3].

Our interest here is in going beyond this mean-field description by considering situations in which the form of the Kac potential $J(r)$, not just its integral $\alpha$, is relevant. To set the stage for the problems that we consider here, we recall some further developments concerning (3) due to Gates and Penrose [3], who related the free energy density $f(n)$ to a mesoscopic variational problem. Such mesoscopic variational problems will be the focus of our attention here.

Let $\mathcal{F}_\Omega(\{\rho\})$ be the mesoscopic free energy functional defined by

$$\mathcal{F}_\Omega(\{\rho\}) = \int_\Omega \left[f_s(\rho(x)) + \frac{1}{2}\int_\Omega \rho(x)J(x-y)\rho(y)\,dy\right]\mathrm{d}x, \tag{5}$$

where $\rho(x)$ is some density profile and let

$$f_\Omega(n) = \frac{1}{|\Omega|}\inf \mathcal{F}_\Omega(\{\rho\}), \tag{6}$$

where the inf is to be taken over all the density profiles $\rho(x)$, $x \in \Omega$, such that

$$\frac{1}{|\Omega|}\int_\Omega \rho(x)\,\mathrm{d}x = n. \tag{7}$$

Then Gates and Penrose showed [3] that

$$f(n) = \lim_{\Omega\to\infty} f_\Omega(n). \tag{8}$$

The function $f_\Omega(n)$ is related directly to the microscopic model even without taking the limit $|\Omega| \to \infty$. Consider $\Omega_\gamma$ to be a scaled up version of a fixed domain $\Omega$, e.g. $\Omega_\gamma$ is a $d$-dimensional cube or torus (i.e. periodic boundary conditions) with sides of length $\gamma^{-1}L$, and let $N_\gamma = n|\Omega_\gamma|$. One has, at least implicitly in the arguments of [2] and with precise estimates on the error bars in [4], that

$$-\beta^{-1}\lim_{\gamma\to 0}\frac{1}{|\Omega_\gamma|}\log Z(N_\gamma,\Omega_\gamma) = f_\Omega(n). \tag{9}$$

To understand the relation between the variational formulation and the convex envelope construction (3), consider the case where $J(x) \le 0$ and of finite range, $J(x) = 0$ for $|x| > R$. Then for a periodic box $\Omega$, $|\Omega| = L^d$, with $L \ge 2R$, we have

$$\mathcal{F}_\Omega(\{\rho\}) = \left\{\int_\Omega\left[f_s(\rho) + \frac{1}{2}\alpha\rho^2(x)\right]\mathrm{d}x - \frac{1}{4}\int_\Omega\int_\Omega J(x-y)[\rho(x)-\rho(y)]^2\,\mathrm{d}x\,\mathrm{d}y\right\}. \tag{10}$$

It is clear that whenever $\alpha$ is such that

$$\frac{\mathrm{d}^2}{\mathrm{d}n^2} f_s(n) + \alpha \ge 0$$

for all (permissible) $n$ then the minimizing $\rho(x)$ will be the constant density profile $\rho(x) = n$. This will always be the case for $|\alpha|$ sufficiently small when the temperature is such that the system with only short-range potential $U(r)$ has a strictly convex free energy $f_s''(n) \ge \epsilon > 0$.

If on the other hand $f_s(n)+\frac{1}{2}\alpha n^2$ has a concave part then for values of $n$ in a certain range the minimizing $\rho(x)$ will be non-uniform, corresponding to the system being separated into a high density liquid phase $n_\ell$ and a low density vapour phase $n_v$. The free energy will then be given, in the limit $L\to\infty$, by (3) while for finite $L$ there will be corrections proportional to the surface area separating the two phases (divided by the volume) which correspond to the surface tension. This correction is lost in $f(n,\gamma)$ and thus in $f(n)$, but can be captured by $\mathcal{F}_\Omega(\{\rho\})$ and $f_\Omega(n)$. We are particularly interested here in the surface tension and the shape of these phase segregation boundaries, including the possibility that in some case the minimizing profile $\rho$ might correspond to the 'dissolution' of a droplet of the minority phase [5–8].

The results described above, as well as those to be discussed later, remain unchanged (and the proofs even simplify) if instead of considering particles in the continuum, we consider lattice systems in $\Omega\subset\mathbb{Z}^d$. We can think of the sites as either occupied or unoccupied, as in a lattice gas model, or to spins pointing up or down, as in an Ising model.

A great deal of work has been done developing precise estimates for the probabilities of observing density profiles which differ significantly from the typical ones in such lattice systems and the results are expected to hold also for continuum systems, cf. [4, 9, 10]. The relation between the microscopic configurations and the continuous density profiles considered in (8) is given by a coarse-graining procedure. We will not go into the technicalities concerning the coarse graining that make it possible to refer to the probability, under the canonical probability distribution, of a particular mesoscopic density profile $\rho(x)$ for the scaled microscopic system, $P_{\Omega_\gamma}(\rho_\gamma)$, where $\rho_\gamma(x)=\rho(\gamma^{-1}x)$. The relation between $P_{\Omega_\gamma}(\rho_\gamma)$ and the mesoscopic functional $\mathcal{F}_\Omega$ is given by

$$\lim_{\gamma\to 0}\gamma^d\log P_{\Omega_\gamma}(\rho_\gamma)=-\beta[\mathcal{F}_\Omega(\{\rho\})-|\Omega|f_\Omega(n)] \tag{11}$$

for any density profile $\rho$ satisfying the constraint $\int_\Omega\rho(x)\,dx=n|\Omega|$. In probabilistic terminology, $\beta[\mathcal{F}_\Omega(\{\rho\})-|\Omega|f_\Omega(n)]$ is the large deviation functional for observing a mesoscopic density [9–11]. This was used in [9, 11] to prove that not only the bulk free energy but also the surface tension can be obtained from $f_\Omega$. Indeed, such analysis has provided a rigorous justification of the Wulff construction for the phase segregation boundary in such models.

The lattice gas setting provides certain technical advantages—it automatically provides a simple hard core which makes collapse impossible. This has led to proofs that the behaviour of the system for small $\gamma$ is close to that for $\gamma\to 0$. We expect, however, that everything proved in the lattice setting will also be valid for the continuum, although this has been done at present only for very special models, such as the one considered by Lebowitz *et al.* [12].

Analogous results hold for the free energy (pressure) obtained from the grand-canonical ensemble (in analogy to (2)) at fixed chemical potential $\mu$ [3]. Thus in the limit $\gamma\to 0$

$$\begin{aligned} g_\Omega(\mu)&=\frac{1}{|\Omega|}\inf_{\rho(x)}\left\{\int_\Omega\left[f_s(\rho(x))+\frac{1}{2}\int_\Omega\rho(x)J(x-y)\rho(y)\,dy\right]dx\right.\\ &\qquad\left.-\mu\int_\Omega\rho(x)\,dx\right\}\\ &:=\frac{1}{|\Omega|}\inf_{\rho(x)}\mathcal{G}_\Omega(\{\rho(x)\})=\inf_n[f_\Omega(n)-\mu n], \end{aligned} \tag{12}$$

where the minimization is now done without the constraint (7). The limit $|\Omega|\to\infty$ gives the $g(\mu)=\lim_{\gamma\to 0}g(\mu,\gamma)$. We note that while $f_\Omega(n)$ may not be convex for finite $\Omega$, $g_\Omega(\mu)$ is always a concave function of $\mu$.

The above analysis extends directly to the case of mixtures of $k$-components. One simply replaces $\rho$, $n$ and $\mu$ by vectors $\boldsymbol{\rho}=(\rho_1,\ldots,\rho_k)$, $\boldsymbol{n}=(n_1,\ldots,n_k)$, $\boldsymbol{\mu}=(\mu_1,\ldots,\mu_k)$ and $J$ by a matrix of interactions $J=\{J_{ij}\}$, $i,j=1,\ldots,k$. The structure of the phase diagram of the mixture is much more complex than that of the one-component case and the long range interactions can produce both vapour–liquid and phase segregation transitions. These have been studied on the mean-field level already by van der Waals [13] and by Korteweg [14] (see also [15]).

In section 2 we review briefly some of our earlier work showing how, using the mesoscopic (local mean field) description, one can obtain additional information about the spatial arrangement of the coexisting phases. This is done without knowledge of the surface tension and the shape of the coexisting domains.

In section 3 we go further and describe new results about the shape of coexisting liquid and vapour domains in one-component systems. We do this in the context of the so-called Cahn–Hilliard free energy functional (first considered by van der Waals) where the computations can be done both rigorously and quite explicitly. We consider there, in particular, the case where one of the phases is present in a much smaller amount than the total volume, i.e. $n-n_v$ goes to zero as $|\Omega|\to\infty$. Depending on the amount present, i.e. whether $n-n_v$ is bigger or smaller than $c|\Omega|^{-1/(d+1)}$,

with $c$ a precisely determined constant, the system may either form a liquid droplet or just supersaturate the vapour phase. The result gives a surprisingly accurate picture of the formation of liquid drops in the vapour phase, as compared with exact microscopic computations for the two-dimensional nearest-neighbour Ising model, and clarifies some points raised in the Rowlinson–Widom book [6].

The relation between the Cahn–Hilliard functional and $\mathcal{F}_\Omega(\{\rho\})$ is discussed in section 4.

## 2. The two-component system

We consider a simple two-component system in which the different species interact only by a repulsive pair potential, as in the celebrated Widom–Rowlinson model [16]. There will now be two density profiles $\rho_1(x)$ and $\rho_2(x)$ and the free energy density corresponding to (5) will be

$$\mathcal{F}_\Omega(\{\rho_1,\rho_2\}) = \int_\Omega f_s(\rho_1,\rho_2)\,\mathrm{d}x + \frac{1}{2}\sum_{i,j=1}^{2}\int_\Omega\int_\Omega \rho_i(x)J_{ij}(x-y)\rho_j(y)\,\mathrm{d}y\,\mathrm{d}x. \tag{13}$$

We shall assume that $J_{ij}(x) = J_{ij}(|x|)$ is monotone (decreasing in magnitude) of finite range with $J_{11} = J_{22} \le 0$, while $J_{12}(x) \ge 0$, i.e. there is attraction of the Kac type between particles of the same species and repulsion between particles of different species. For the short-range part we shall assume that $f_s(\rho_1,\rho_2)$ is jointly convex in $\rho_1$ and $\rho_2$ and has the simple form

$$f_s(\rho_1,\rho_2) = \beta^{-1}[F(\rho_1) + F(\rho_2) + D(\rho_1+\rho_2)] \tag{14}$$

with $(\mathrm{d}^2/\mathrm{d}t^2)D(t) \ge 0$. An example of the type of $f_s$ we have in mind is

$$F(t) = t\log t - t,$$
$$D(t) = \begin{cases} -t\log(1-bt), & x < b^{-1}, \\ +\infty, & x < b^{-1}. \end{cases} \tag{15}$$

To obtain $f_\Omega(n_1,n_2)$ we have to minimize $\mathcal{F}_\Omega(\rho_1,\rho_2)$ over $\rho_1(x)$ and $\rho_2(x)$ subject to the constraints

$$\frac{1}{|\Omega|}\int_\Omega \rho_1(x)\,\mathrm{d}x = n_1, \quad \frac{1}{|\Omega|}\int_\Omega \rho_2(x)\,\mathrm{d}x = n_2. \tag{16}$$

In the limit $|\Omega| \to \infty$ we obtain, in analogy to (3),

$$f(n_1,n_2) = CE\left[f_s(n_1,n_2) + \frac{1}{2}\sum_{ij=1}^{2}\alpha_{ij}n_in_j\right] \tag{17}$$

with

$$\alpha_{ij} = \int_{\mathbb{R}^d} J_{ij}(x)\,\mathrm{d}x, \tag{18}$$

and where $CEf_\Omega(n_1,n_2)$ denotes the maximal convex function lying below $f_\Omega$.

Depending on the values of the $\alpha_{ij}$ this system can exist either in a single homogeneous phase, or in as many as four coexisting phases consisting of a fluid and a vapour each segregated into a species 1 rich and a species 2 rich phase [17].

The main tool used in [17] to analyse the phase diagram of this system is a 'rearrangement inequality' refining a classical one proved in [18]. Let $\Omega$ be a torus with $|\Omega| = L^d$ and $L > 2R$, $R$ being the range of $J_{ij}(x)$. We then have that the minimizing profiles $\bar\rho_i(x)$, $i=1,2$, are monotone along each coordinate of the torus. Put another way, let $x=0$ be the position of the maximum of $\bar\rho_1(x)$, then $\bar\rho_1(x)$ will be symmetric decreasing in the coordinates $x_\alpha$, $\alpha = 1,\ldots,d$, reaching its minimum at $x_\alpha = L/2$ (the same as $x_\alpha = -L/2$) for all $\alpha$. The density $\bar\rho_2(x)$ will behave in the opposite way, having its minimum at $x=0$ and its maximum at $x_\alpha = L/2$. It follows from this that there are certain relations between the possible densities in the case of coexistence of four phases, a segregated liquid with total bulk density $\rho_\ell$ and a segregated vapour with total density $\rho_v$. Let $\rho_\ell^+(\rho_\ell^-)$ be the density of the majority (minority) species in the liquid phase and similarly $\rho_v^\pm$ in the vapour phase, with $\rho_\ell = \rho_\ell^+ + \rho_\ell^- > \rho_v^+ + \rho_v^-$. Then our theorem in [17] states that the densities must satisfy the inequalities

$$\rho_\ell^- \le \rho_v^- \le \rho_v^+ \le \rho_\ell^+. \tag{19}$$

We show in figure 1, taken from [17], a schematic diagram of the four phases on the two-dimensional torus. Region A corresponds to $\rho_1 = \rho_\ell^+$, region B to $\rho_1 = \rho_v^+$, region C to $\rho_1 = \rho_v^-$ and region D to $\rho_1 = \rho_\ell^-$. Thus the high density liquid region which has a smaller volume is split up into two regions A and D.

The inequalities (19) and the corresponding arrangement of phases in figure 1 have been obtained without calculating the different surface tensions. The actual shapes of the regions given in figure 1 are based on the assumption that they are controlled by a surface tension

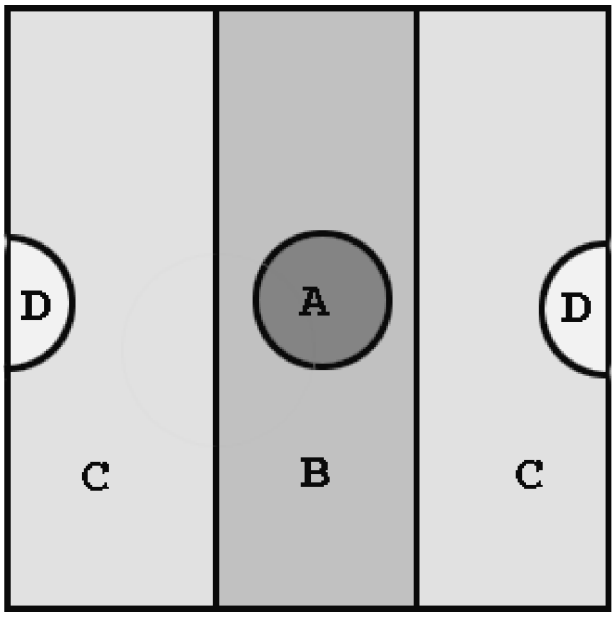


Figure 1. Schematic picture of coexisting phases.

which wants to minimize the length of the boundaries between the different phases.

The surface tension terms will give corrections to the bulk approximation provided by

$$\inf_{\rho_1,\rho_2} \mathcal{F}_\Omega(\{\rho_1,\rho_2\}) \approx |\Omega| f_\Omega(n_1,n_2). \tag{20}$$

We expect that

$$\inf_{\rho_1,\rho_2} \mathcal{F}_\Omega(\{\rho_1,\rho_2\}) = f_\Omega(n_1,n_2)|\Omega| + b(n_1,n_2)|\Omega|^{1-1/d} + \text{lower order terms.} \tag{21}$$

The coefficient $b$ specifying the next corrections will be given by

$$b(n_1,n_2) = \lim_{|\Omega|\to\infty} \frac{\inf_\rho \mathcal{F}_\Omega(\{\rho_1,\rho_2\}) - |\Omega| f_\Omega(n_1,\, n_2)}{|\Omega|^{1-1/d}}, \tag{22}$$

should this limit exist. This has indeed been proved for one-component systems and is undoubtedly true also in the present case. In fact, one can go beyond the leading order given in (22) if one considers further simplifications of the model mesoscopic free energy. This is what we do in the next section.

## 3. Surface tension and droplet formation

The problem of computing the corrections to the free energy described in (21) is quite challenging for non-local $\mathcal{F}$'s of form (13) or (10). We therefore turn now to the consideration of a simplified one-component free energy functional that captures the essential features of the non-local functional (10), namely the Cahn–Hilliard or Landau–Ginzburg functional

$$\tilde{\mathcal{F}}_\Omega(\{m\}) = \int_\Omega \left( \frac{\theta^2}{2} |\nabla m|^2 + F(m(x)) \right) \mathrm{d}x, \tag{23}$$

where $F(t) = (t^2-1)^2/4$ is a symmetric double well potential which has minima at $t = \pm 1$. The function $m(x)$ is a real-valued order parameter field, e.g. the magnetization of an Ising spin system, which plays the same role as the density.

The parameter $\theta$ has the dimensions of a length; it measures the thickness of an interface between regions of phase $+1$ and $-1$. The interaction term in $\tilde{\mathcal{F}}_\Omega$ is expressed in terms of the gradient which affords us several technical advantages. The connection between $\tilde{\mathcal{F}}$ and $\mathcal{F}$ will be discussed in section 4.

We now turn to the problem of finding the minimizers arising in the computation of

$$\tilde{f}_\Omega(n) = \frac{1}{|\Omega|} \inf \left\{ \tilde{\mathcal{F}}_\Omega(\{m\}) \colon m \in \mathcal{M}_n \right\}, \tag{24}$$

with $\mathcal{M}_n$ the set of functions $m$ on $\Omega$ such that

$$\frac{1}{|\Omega|} \int_\Omega m(x)\, \mathrm{d}x = n. \tag{25}$$

Since $m$, unlike $\rho$, is real valued, both positive and negative values of $n$ are physically meaningful.

A simple compactness argument [19] shows that such minimizers exist and satisfy the Euler–Lagrange equation

$$-\theta^2 \Delta m(x) + F'(m(x)) + \mu = 0, \tag{26}$$

where $\mu$ is a Lagrange multiplier (or chemical potential) associated with the constraint (25): $\Delta = \nabla^2$ is the Laplace operator.

For $\theta = 0$ and $-1 \le n \le 1$, the minimization problem is trivial: there will be a region $A$ in $\Omega$ with $m(x) = 1$ on $A$ and $m(x) = -1$ on the complement of $A$. Let $|A|$

denote the volume of $A$. Then, from (25),

$$n = -1 + 2\frac{|A|}{|\Omega|}. \tag{27}$$

Note that when $-1 \le n \le 1$, the chemical potential $\mu$ is zero. Solving for $|A|$, we have

$$|A| = |\Omega|\frac{n+1}{2}. \tag{28}$$

For large values of $\theta$, the functional $\tilde{\mathcal{F}}_\Omega$ is strictly convex and then the problem is also trivial: when $\tilde{\mathcal{F}}_\Omega$ is strictly convex, the unique minimizer will be the constant function $m(x) = n$. The spectral gap, i.e. the first eigenvalue above zero, for the operator $-\Delta$ on $\Omega$ is $(2\pi/L)^d$ and since $F''(t) = 3t^2 - 1 \ge -1$, $\tilde{\mathcal{F}}_\Omega$ is certainly strictly convex for $\theta > L/(2\pi)$; i.e. there will be no phase segregation if the system is confined to a domain which is small compared to the range of the interaction responsible for the transition.

What we are interested in is what happens for values of $\theta$ small compared to $L$. For such values of $\theta$, we expect the minimizer to exhibit both phases, as with $\theta = 0$, but now we have to pay a price for making the transition across the boundary of $A$, so that $A$ should have a minimal surface given its volume in (28). The solution of the isoperimetric problem on the torus depends on $|A|/|\Omega|$. For $|A|/|\Omega|$ sufficiently small it is given by taking a sphere. For $|A|/|\Omega|$ sufficiently large it is given by a slab. See [19] for further discussion.

The *equimolar radius*, $r_0$, is defined to be the radius of the sphere whose volume is $|A|$, as in (28). As a function of $n$, it is given by

$$r_0 = \left(\frac{n+1}{2\sigma(d)}\right)^{1/d} L. \tag{29}$$

One can also guess the profile of the transition across the boundary of $A$ for a minimizer and the value of $f_\Omega(n)$ for small values of $\theta$.

To do this, let us consider a planar interface in a long cylinder with one end deep in the region where $m \approx 1$ and the other deep in the region where $m \approx -1$. Let $z$ be the coordinate running along the cylinder. The computation of the minimal excess free energy per unit area in such a cylinder is a one-dimensional problem and taking the length to infinity, we are led to consider, for $\theta > 0$, the quantity $S$ defined by

$$\frac{S}{\theta} = \inf\left\{ \int_{\mathbb{R}} \left(\frac{1}{2}|m'(z)|^2 + F(m(z))\,\mathrm{d}z\right) : \lim_{z\to\pm\infty} m(z) = \mp 1 \right\}, \tag{30}$$

where $z$ is measured in units of $\theta$.

Let $\bar{m}$ denote the antisymmetric minimizer for this variational problem.

For the particular functional (24), this minimizer is given by the well-known hyperbolic tangent of Van der Waals [13],

$$\bar{m}(z) = -\tanh\left(z/2^{1/2}\right), \tag{31}$$

from which $S$ can be computed. It is useful to note that

$$S = 2\theta \int_{\mathbb{R}} \frac{1}{2}|\bar{m}'(z)|^2\,\mathrm{d}z = 2\theta \int_{\mathbb{R}} F(\bar{m}(z))\,\mathrm{d}z. \tag{32}$$

Using the planar transition profile $\bar{m}$, one constructs a natural trial function for the minimization problem (24) when the curvature of the interface is small compared to the thickness $\theta$. Let $\Gamma$ be the surface of minimal area bounding a region $A$ with $|A|$ satisfying (27). Assume that $|A|/|\Omega|$ is sufficiently small, so that $\Gamma$ is a sphere of radius $r_0$. Let $d(x, \Gamma)$ denote the signed distance function, so that $d(x, \Gamma)$ is the distance from $x$ to $\Gamma$ if $x$ is in the interior, i.e. $A$, and is minus the distance from $x$ to $\Gamma$ if $x$ is in the exterior.

The natural trial function is then

$$m_0(x) = \bar{m}\left(\frac{d(x,\Gamma)}{\theta}\right). \tag{33}$$

Computing $\tilde{\mathcal{F}}_\Omega(\{m_0\})$ using spherical coordinates near $\Gamma$, we find

$$\tilde{\mathcal{F}}_\Omega(\{m_0\}) = S|\Gamma| + O(\theta^2), \tag{34}$$

where $|\Gamma| = \mathrm{d}\sigma(d) r_0^{d-1}$ is the surface of the sphere with equimolar radius $r_0$. This means that to leading order in $\theta$, the surface tension is just that given by the planar interface.

### 3.1. *Droplet formation versus evaporation*

It is not the case that (33) is even an approximate minimizer for all values of $n$. If $n$ is sufficiently small, then the droplet will 'evaporate': it costs less free energy to spread $m$ uniformly over $\Omega$ than it does to form the interface required to separate $m$ into the two minimizing phases.

To see this, consider as an alternative the constant function $m(x) = n$: we obtain from (27) and the fact that $F(-1) = F'(-1) = 0$,

$$\tilde{\mathcal{F}}_\Omega(n) = \frac{1}{2}F''(-1)\left(\frac{2|A|}{|\Omega|}\right)^2 |\Omega| + O\left(|\Omega|^{-2}|A|^3\right). \tag{35}$$

Introducing the *compressibility* $\chi$ by

$$\chi^{-1} = F''(-1) = F''(1), \tag{36}$$

we have

$$\tilde{\mathcal{F}}_\Omega(n) = 2\frac{\sigma(d)^2 r_0^{2d}}{\chi|\Omega|} + \mathcal{O}\big(|\Omega|^{-2}|A|^3\big). \tag{37}$$

Comparing this with (34) we see that the droplet trial function is favoured only in the case

$$2\frac{\sigma(d)^2 r_0^{2d}}{\chi|\Omega|} > S\,\mathrm{d}\sigma(d) r_0^{d-1}. \tag{38}$$

Note that if $r_0$ and $L$ are related by

$$r_0 = \delta^{1/d} L^{\nu}, \tag{39}$$

then (38) is satisfied independently of $\delta$ for all large $L$ provided $\nu > d/(d+1)$ and is violated independently of $\delta$ for all large $L$ whenever $\nu < d/(d+1)$.

Therefore, if in our minimization problem (24), $n$ is related to $L$ through

$$\frac{n+1}{2} = \sigma(d)\delta L^{d\nu - d} \tag{40}$$

which corresponds to (39) through (29), we expect to have, for all large $L$, droplet type minimizers for $\nu > d/(d+1)$ and uniform minimizers for $\nu < d/(d+1)$.

Our goal here is to determine the nature of the droplet type minimizers for all values of $\nu$ up to and including the critical value $\nu = d/(d+1)$. We can do this by using a Chapman–Enskog–Hilbert type expansion to solve the Euler–Lagrange equation (26). The dimensionless quantity

$$\lambda = \frac{\theta}{r_0}, \tag{41}$$

where $r_0$ is the equimolar radius, will be the expansion parameter. This is just the ratio of the intrinsic interface thickness to the radius of the droplet.

We make the following prescription to specify the expansion.

(1) The interfacial surface $\Gamma_\lambda$ will be a sphere of radius $r(\lambda)$ where

$$r(\lambda) = r_0 + \lambda r_1 + O(\lambda^2) := r^{(1)} + O(\lambda^2). \tag{42}$$

The fact that it is a sphere actually comes out of the analysis.

(2) The Lagrange multiplier (chemical potential) $\mu$ appearing in (26) has an expansion of the form

$$\mu(\lambda) = \lambda\mu_1 + O(\lambda^2). \tag{43}$$

Recall that $\mu = 0$ for $\theta = 0$, which is why $\mu(0) = 0$.

(3)

$$m_\lambda(x) = \bar{m}\left(\frac{d(x,\Gamma^{(1)})}{\theta}\right) + \lambda(h_1(x) + \phi_1) + O(\lambda^2) := m^{(1)} + O(\lambda^2), \tag{44}$$

where $\phi_1$ will be at least asymptotically constant and $h_1$ is a function that decays to zero exponentially away from the interface.

(4) We require that the constraint (25) be approximately satisfied in the sense that

$$\frac{1}{|\Omega|}\int_\Omega m^{(1)}(r)\,\mathrm{d}r = n + O\big(\lambda^2\big). \tag{45}$$

With $z = d(x,\Gamma)/\theta$, we can write the Laplacian as

$$\theta^2\Delta = \frac{\mathrm{d}^2}{\mathrm{d}z^2} + (d-1)\lambda K\frac{\mathrm{d}}{\mathrm{d}z} + O(\lambda^2), \tag{46}$$

where $K = r_0/r(\lambda)$ is the mean curvature of the sphere $\Gamma_\lambda$ in units of $r_0$. Then, substituting the above expansions in (26) we get at order zero in $\lambda$

$$-\bar{m}'' + F'(\bar{m}) = 0 \tag{47}$$

and at the first order

$$-(d-1)K\bar{m}' - h_1'' + F''(\bar{m})h_1 + F''(\bar{m})\phi_1 + \mu_1 = 0. \tag{48}$$

Hence, if we can find $\bar{m}$, $h_1$, $\phi_1$ and $\Gamma^{(1)}$ so that the previous equations are satisfied we have that $m_\lambda$ is an approximate solution to (26) in the sense that

$$-\Delta m^{(1)}(x) + F'(m^{(1)}(x)) + \lambda\mu_1 = O(\lambda^2)\ , \tag{49}$$

We choose as $\bar{m}$ the front with asymptotic values $\pm 1$ at infinity, i.e.

$$\bar{m}(z) = -\tanh(z/2^{1/2}), \tag{50}$$

and define the operator $\mathcal{L}$ by

$$\mathcal{L} = -\frac{\mathrm{d}^2}{\mathrm{d}z^2} + F''(\bar{m}). \tag{51}$$

Then we can rewrite (48) as

$$\mathcal{L}h_1 = (d-1)K\bar{m}' - (F''(\bar{m})\phi_1 + \mu_1). \tag{52}$$

The null space of $\mathcal{L}$ is spanned by $\bar{m}'$, and so, by the Fredholm criterion, (52) is solvable provided that $(d-1)K\bar{m}' - (F''(\bar{m})\phi_1 + \mu_1)$ is orthogonal to $\bar{m}'$.

In order to check this condition we multiply the right-hand side of (52) by $\bar{m}'$ and integrate in $\mathrm{d}z$. Using the fact that $\int_{\mathbb{R}} F''(\bar{m})\bar{m}'\,\mathrm{d}z = 0$ and $\int_{\mathbb{R}} \bar{m}'\,\mathrm{d}z = -2$ yields

$$(d-1)K\left(\int_{\mathbb{R}} (\bar{m}')^2\,\mathrm{d}z\right) = -2\mu_1. \tag{53}$$

Using (32) to express the integral in terms of $S$, we obtain

$$\mu_1 = -\frac{1}{2}(d-1)K\frac{S}{\theta}. \tag{54}$$

Next, to determine $\phi_1$, note that if the right-hand side of (52) has to decay to zero for large $|z|$, necessarily

$$\lim_{|z|\to\infty} [(d-1)K\bar{m}' - (F''(\bar{m})\phi_1 + \mu_1)] = 0. \tag{55}$$

Since $\lim_{|z|\to\infty} \bar{m}'(z) = 0$ and $\lim_{|z|\to\infty} F''(\bar{m}(z)) = F''(1) = \chi^{-1}$, we have

$$\chi^{-1}\phi_1 + \mu_1 = 0, \tag{56}$$

that is,

$$\phi_1 = -\chi\mu_1 = \frac{(d-1)\chi KS}{2\theta}. \tag{57}$$

Using (54) and (57), (52) becomes

$$\mathcal{L}h_1 = (d-1)K\left(\bar{m}' - \frac{S}{2}(1 - \chi F''(\bar{m}))\right). \tag{58}$$

The right-hand side is rapidly decaying and so there is a unique rapidly decaying solution $h_1$. It is not difficult to realize that $h_1$ is indeed identically zero.

Finally, we determine the radius of the droplet, $R = r^{(1)}$, using the approximate constraint (45). Since $h_1$ is zero we get that $m^{(1)} = \bar{m} + \lambda\phi_1$ and

$$\begin{aligned}\int_\Omega m^{(1)}(x)\,\mathrm{d}x &= -|\Omega| + 2\sigma(d)R^d + \lambda|\Omega|\phi_1 + O(\lambda^2|\Gamma|)\\ &= -|\Omega| + 2\sigma(d)R^d\\ &\quad + \lambda|\Omega|\frac{SK\chi(d-1)}{2\theta} + O(\lambda^2|\Gamma|).\end{aligned} \tag{59}$$

This yields

$$2\sigma(d)R^d + \lambda|\Omega|\frac{SK\chi(d-1)}{2\theta} = 2\sigma(d)r_0^d.$$

We assume that both $r_0$ and $R = r_0 + \lambda r_1$ are proportional to $L^\nu$, according to (39) and we put

$$R = \eta^{1/d}r_0 = \eta^{1/d}\delta^{1/d}L^\nu. \tag{60}$$

Then, recalling that $|\Omega| = L^d$, we obtain an equation for $\eta$,

$$2(\eta - 1) + \frac{d-1}{d}\omega^{-1}\eta^{-1/d}L^{d-\nu(d+1)} = 0, \tag{61}$$

where we have introduced the parameter

$$\omega = \frac{2\sigma(d)\delta^{(d+1)/d}}{d\chi S} \tag{62}$$

for future convenience.

If $\nu > d/(d+1)$ the exponent of $L$ is negative so that for $L$ large we can solve approximately the equation and get

$$\eta = 1 - \epsilon\frac{d-1}{2d\omega} + O(\epsilon^2) \tag{63}$$

with

$$\epsilon = L^{d-\nu(d+1)} \tag{64}$$

so that the correction to the equimolar radius is small when the volume is large.

If $\nu$ takes the critical value $\nu = d/(d+1)$ the equation (61) becomes independent of $L$, yielding

$$2(\eta - 1)\omega + \frac{d-1}{d}\eta^{-(1/d)} = 0. \tag{65}$$

We need to solve (64) for $\eta$ in order to find the size of the spherical droplet. We can get some idea of the solutions by the following remark: let us compute the free energy corresponding to the approximate solution $m^{(1)}$. We have

$$\int_\Omega |\nabla(\bar{m}+\lambda\phi_1)|^2\,\mathrm{d}x = \int_\Omega |\nabla\bar{m}|^2\,\mathrm{d}x \;= \frac{1}{2}S|\Gamma|,$$

$$\int_\Omega F(m_\lambda)\,\mathrm{d}x = \left(\int_{\mathbb{R}} F(\bar{m}(z))\,\mathrm{d}z\right)|\Gamma| + \frac{1}{2\chi}\phi_1^2\lambda^2 L^d + O(1). \tag{66}$$

Therefore,

$$\tilde{\mathcal{F}}(\{m_\lambda\}) = S|\Gamma| + \frac{1}{2\chi}\lambda^2 L^d\phi_1^2 + O(1) := \mathcal{F}_{\mathrm{drop}} + O(1). \tag{67}$$

Next, we rewrite $\mathcal{F}_{\mathrm{drop}}$ in terms of the parameters $\eta$, $\delta$, $\omega$. By (59) we get

$$\phi_1 = \frac{2}{\lambda L^d}(1-\eta)\sigma(d)r_0^d. \tag{68}$$

Hence

$$\mathcal{F}_{\mathrm{drop}}(\eta) = \mathrm{d}\sigma(d)r_0^{d-1}S\left[\eta^{(d-1)/d} + \frac{1}{\chi Sd}(1-\eta)^2 2\sigma(d)\frac{r_0^{d+1}}{L^d}\right]. \tag{69}$$

Therefore, setting $|\Gamma_0| = d\sigma(d)r_0^{d-1}$, the droplet free energy as a function of the droplet size $\eta$ in units $r_0$ is given by

$$\mathcal{F}_{\mathrm{drop}}(\eta) = S|\Gamma_0|[\eta^{(d-1)/d} + (1-\eta)^2\omega]. \tag{70}$$

The relevance of the function $\Phi(\eta) = \eta^{(d-1)/d} + (1-\eta)^2\omega$ to the issue of small droplet formation was first pointed out in [20]. There they gave a heuristic argument that the droplet would form when $\inf_\eta \Phi(\eta) < \Phi(0)$. Whether this happens or not depends on the value of $\omega$. If

$$\omega < \omega_{\mathrm{c}} = \frac{1}{d}\left(\frac{d+1}{d}\right)^{(d+1)/d}, \tag{71}$$

the minimal value of $\Phi(\eta)$ is achieved for $\eta = 0$ and this corresponds to the free energy of the homogeneous state with the prescribed value of $n$. If $\omega > \omega_{\mathrm{c}}$ then the minimizer is non-homogeneous and corresponds to the formation of a droplet. This heuristic picture was rigorously justified in [20] in the case of the two-dimensional nearest-neighbours Ising model.

We can prove in [19] that the same critical value for $\omega$ governs the formation of small droplets for the Cahn–Hilliard free energy functional. Moreover we show there that in the regime where the minimizers are not uniform, they correspond to droplets whose shape is spherical with radius $R$ given by (60) with $\eta$ being the largest solution to (65) for a given $\omega \geq \omega_{\mathrm{c}}$. This result allows one to accurately draw a picture analogous to [20] for the Cahn–Hilliard free energy functional.

Our proof in [19] is based on the the construction of upper and lower bounds for the free energy. The upper bound just follows from choosing the trial function $m^{(1)}$ with $r^{(1)}$ solving (65) which is a consequence of the mass constraint and is just the condition in order that $\eta$ be a critical value for $\mathcal{F}_{\mathrm{drop}}(\eta)$.

In proving the lower bound we use the co-area formula of geometric measure theory and this is made possible by the fact that the interaction is local and expressed in terms of the gradient of the order parameter.

## 4. Concluding remarks

There is a close formal connection between the Cahn–Hilliard free energy functional and the non-local free energy functionals derived from $\gamma \to 0$ considered in the first two sections. This leads us to expect that it will be possible to extend the analysis of small droplet formation to the multicomponent, non-local setting of section 2.

Making the change of variables $m(x) = 2\rho(x) - 1$ and setting $J \to 8J$, $\alpha = 8\alpha$, the free energy function $\mathcal{F}_\Omega$ defined in (10) becomes, up to constant terms,

$$\mathcal{F}_\Omega(\{(1+m)/2\}) = \int_\Omega \big(f_{\mathrm{s}}(m(x)) + \alpha m^2(x)\big)\,\mathrm{d}x - \frac{1}{2}\int_\Omega\int_\Omega J(x-y)(m(x)-m(y))^2\,\mathrm{d}x\,\mathrm{d}y, \tag{72}$$

where we keep denoting the short-range free energy density by $f_{\mathrm{s}}$ although now it is a function of $m$ rather than $\rho$.

For $J < 0$, the term $(-1/2)\int_\Omega \int_\Omega J(x-y)(m(x)-m(y))^2\,\mathrm{d}x\,\mathrm{d}y$ penalizes variations in $m$. One might then expect that for any function $m$ that nearly minimizes $\mathcal{F}_\Omega$, the first-order Taylor approximation

$$m(y) \approx m(x) + \nabla m(x)\cdot(y-x) \tag{73}$$

should not be too terribly crude. Making this approximation,

$$-\int_\Omega\int_\Omega J(x-y)(m(x)-m(y))^2\,\mathrm{d}x\,\mathrm{d}y \approx \theta^2\int_\Omega |\nabla m(x)|^2\,\mathrm{d}x, \tag{74}$$

with $\theta^2 = -\int_{\mathbb{R}^d} x^2 J(x)\,\mathrm{d}x$, leads to the Cahn–Hilliard type free energy functional

$$\theta^2\int_\Omega |\nabla m(x)|^2\,\mathrm{d}x + \int_\Omega \big(f_s(m(x)) + \alpha m^2(x)\big)\mathrm{d}x. \tag{75}$$

When $\alpha$ is sufficiently negative, $(f_s(m)+\alpha m^2)$ is a double-well potential whose essential features are represented by $F(m) = (m^2-1)^2/4$, and thus we have arrived at $\tilde{\mathcal{F}}_\Omega$.

Despite the rather direct connection between $\tilde{\mathcal{F}}_\Omega$ and $\mathcal{F}_\Omega$, it is not so obvious how to directly treat nonlocal interactions. The construction of the very precise trial function, based on the Chapman–Enskog–Hilbert expansion, that was used here for the upper bound, can be carried to arbitrary order. It is reasonable to expect that it is essentially a calculation of the minimizers of $\mathcal{F}$. However, our proof in the Cahn–Hilliard case makes use of the gradients in $\tilde{\mathcal{F}}_\Omega$.

We remark finally that in the Kac models considered here the mesoscopic free energy functional, described by (6) and (12) is derived from a separation of scales between the interparticle spacing and the range of the Kac potential $\gamma^{-1}$. In the units used for $f_\Omega$ and $g_\Omega$ the interparticle distance, which is also the scale of the short-range interaction, is of order $\gamma$, which is being taken to zero in this limit. A deeper analysis, such as provided by the renormalization group, should be able to give effective mesoscopic free energies for systems with short-range potentials. The use of mesoscopic free energies forms the basis of density functional theory which is quite successful. We are however far from being able to do this rigorously.

## Acknowledgements

We thank T. Bodineau, E. Presutti and B. Widom for helpful discussions. The authors would like to thank Professor J.P. Bourguignon for the kind hospitality of IHES, Bures-sur-Yvette, France. EC was partially supported by US NSF grant DMS 03-00349. MCC was partially supported by FCT. RM and RE were partially supported by MIUR, INDAM-GNFM. JLL was supported by AFOSR grant AF-FA9550-04 and NSF Grant DMR 01-279-26.

This work has been achieved thanks to the support of the European Commission through its 6th Framework Program 'Structuring the European Research Area' and the contract No. RITA-CT-2004-505493 for the provision of Transnational Access implemented as Specific Support Action.

## References

[1] D. Ruelle. *Statistical Mechanics: Rigorous Results*, Benjamin, New York (1969), reprinted World Scientific, Singapore (1999); M.E. Fisher. *Arch. Ration. Mech. Anal.*, **17**, 377 (1964); C.J. Thompson. *Mathematical Statistical Mechanics*, Macmillan, New York (1972).

[2] J.L. Lebowitz, O. Penrose. *J. Math. Phys.*, **7**, 98 (1966); see also P.C. Hemmer, J.L. Lebowitz. In *Phase Transitions and Critical Phenomena*, Vol. 5B, C. Domb, L. Green (Eds), Academic Press, New York (1976).

[3] D.J. Gates, O. Penrose. *Commun. Math. Phys.*, **15**, 255 (1969).

[4] E. Presutti. From Statistical Mechanics towards Continuum Mechanics, Notes of Lectures given at Max Planck Institute of Leipzig (1999).

[5] N.G. Hadjiconstantinou, A.L. Garcia, B.J. Alder. *Physica A*, **281**, 337 (2000).

[6] J.S. Rowlinson, B. Widom. *Molecular Theory of Capillarity*, Oxford University Press, Oxford (1982) and Dover, New York (2003).

[7] K. Binder, M.H. Kalos. *J. Stat. Phys.*, **22**, 363 (1990).

[8] M.P.A. Fisher, M. Wortis. *Phys. Rev.* B, **29**, 6252 (1984).

[9] O. Benois, T. Bodineau, E. Presutti. *Stochastic Process. Appl.*, **75**, 89 (1998).

[10] P. Dupuis, R.S. Ellis, *A Weak Convergence Approach to the Theory of Large Deviations*, Wiley Series in Probability and Statistics, John Wiley & Sons, Inc., New York (1997).

[11] O. Benois, T. Bodineau, P. Butta, E. Presutti. *Markov Process. Appl. 3*, **2**, 175 (1997).

[12] J.L. Lebowitz, A. Mazel, E. Presutti. *J. Stat. Phys.*, **94**, 955 (1999).

[13] J.D. van der Waals. *Verhandelingen Kon. Akad. Wet. Amsterdam*, **1**, 1 (1893) [English translation by J.S. Rowlinson. *J. Stat. Phys.*, **20**, 197 (1979)]; see also J.D. van der Waals. In *Studies in Statistical Mechanics*, Vol. IXV, J.L. Lebowitz (Ed.), North Holland, Amsterdam (1988).

[14] D.J. Korteweg. *Arch. Néerl.*, **24**, 57 (1891); *Arch. Néerl.*, **24**, 295 (1891).

[15] J.M.H. Levelt Sengers. *How Fluids Unmix; Discoveries by the School of Van der Waals and Kamerlingh Onnes*, Edita, Amsterdam (2003).

[16] B. Widom, J.S. Rowlinson. *J. Chem. Phys.*, **52**, 1670 (1970).
[17] E. Carlen, M. Carvalho, R. Esposito, J.L. Lebowitz, R. Marra. *Nonlinearity*, **16**, 1075 (2003).
[18] F. Almgren, E. Lieb. *J. Am. Math. Soc.*, **2**, 683 (1989).
[19] E.A. Carlen, M.C. Carvalho, R. Esposito, J.L. Lebowitz, R. Marra. Droplet formation for the Cahn–Hilliard free energy functional, submitted to *J. Geom. Analysis*.
[20] M. Biskup, L. Chayes, R. Kotecky. *Commun. Math. Phys.*, **242**, 137 (2003); *Europhys. Lett.*, **60**, 21 (2002).